

Managing Large Scale Energy Storage Units to Mitigate High Wind Penetration Challenges

Hamideh Bitaraf, *Student Member, IEEE*, Haiwang Zhong, *Member, IEEE*, and Saifur Rahman, *Fellow, IEEE*
 Bradley Department of Electrical and Computer Engineering and Advanced Research Institute
 Virginia Tech
 Arlington, Virginia, USA

Abstract—Due to its intermittent nature, high wind penetration requires more flexibility in the electric power grid to provide the balance. Large scale energy storage is one such option that allows the intermittency to be absorbed in real time. Two types of large scale energy storage technologies including Sodium Sulphur (NaS) battery and compressed air energy storage (CAES) are studied in this paper. In this paper CAES is modeled and evaluated as a large-scale mechanical energy storage unit highlighting its various operational characteristics. This paper focuses on how to maximize the wind energy penetration level while satisfying all the system constraints including wind spill energy constraint and power balance equations. This problem is solved considering different combinations of CAES and NaS battery scenarios. The problem is formulated as a mixed integer linear programming (MILP) solved by CPLEX. To showcase the applicability of the proposed approach, a simulation case study based on a real-world 15-minute interval wind data from Bonneville Power Administration (BPA) in 2013 is presented.

Index Terms—wind power, large scale energy storage, Sodium Sulphur (NaS) battery, Compressed air energy storage (CAES), maximum wind penetration level, mixed integer linear programming (MILP).

NOMENCLATURE

A. Indices

t : Index of time intervals, 15 minutes an interval.

B. Variables

$P_{Cchg,t}$: Continuous variable denoting the quantity of charging power for CAES at time t .

$P_{Cdchg,t}$: Continuous variable denoting the quantity of discharging power for CAES at time t .

$\alpha_{C,t}$: Binary variable denoting whether CAES is charged at time t ; 1 if charged, 0 otherwise.

$\beta_{C,t}$: Binary variable denoting whether CAES is discharged at time t ; 1 if discharged, 0 otherwise.

$\gamma_{C,t}$: Binary variable denoting whether CAES is idle at time t ; 1 if idle, 0 otherwise.

$\rho_{C,t}$: Binary variable denoting the starting indicator of idle modes at time t ; if $\gamma_{N,t} = 1$ and $\gamma_{N,t-1} = 0$, then $\rho_{C,t} = 1$,

$\varphi_{C,t}$: Binary variable denoting the stopping indicator of Idle at time t ; if $\gamma_{N,t} = 0$ and $\gamma_{N,t-1} = 1$, then $\varphi_{C,t} = 1$,

$P_{Nchg,t}$: Continuous variable denoting the quantity of charging power for NaS at time t .

$P_{Ndchg,t}$: Continuous variable denoting the quantity of discharging power for NaS at time t .

$P_{th,t}$: Continuous variable denoting the quantity of thermal unit generation at time t .

$u_{th,t}$: Binary variable denoting whether thermal unit is on or off at time t ; 1 if on, 0 otherwise.

$y_{th,t}$: Binary variable denoting the starting indicator of thermal unit start up at time t ; if $u_{th,t} = 1$ and $u_{th,t-1} = 0$, then $y_{th,t} = 1$,

$z_{th,t}$: Binary variable denoting the stopping indicator of thermal unit shutdown at time t ; if $u_{th,t} = 0$ and $u_{th,t-1} = 1$, then $z_{th,t} = 1$,

$P_{w,t}$: Continuous variable denoting the quantity of wind generation at time t .

$P_{l,t}$: Continuous variable denoting the quantity of load at time t .

$P_{ws,t}$: Continuous variable denoting the quantity of Wind spill power at time t .

μ_w : Wind power scaling factor

C. Parameters

P_C : Rated power capacity for CAES

E_C : Rated energy capacity for CAES

SoC_C^i : Initial state of charge for CAES

η_C : Roundtrip efficiency for CAES

dP_C : Energy storage ramp rates for CAES

This work was supported in part by the U.S. National Science Foundation under grant OISE-1104023.

H. Bitaraf is with Virginia Tech – Advanced Research Institute, Arlington, VA 22203 USA (e-mail: bhamideh@vt.edu).

H. Zhong is with Department of Electrical Engineering, Tsinghua University, Beijing, 100084, China. He is also a visiting scholar at Virginia Tech – Advanced Research Institute, Arlington, VA 22203 USA (e-mail: zhonghw@mail.tsinghua.edu.cn).

S. Rahman is professor and director of Virginia Tech – Advanced Research Institute, Arlington, VA 22203 USA (e-mail: srahman@vt.edu).

T_C^{\min}	: Minimum duration of idle modes for CAES
N_C	: Number of CAES units
P_N	: Rated power capacity for NaS
E_N	: Rated energy capacity for NaS
SoC_N^{\max}	: Maximum state of charge for NaS
SoC_N^{\min}	: Minimum state of charge for NaS
SoC_N^i	: Initial state of charge for NaS
η_N	: Roundtrip efficiency for NaS
dP_N	: Energy storage ramp rates for NaS
N_N	: Number of NaS battery units
dP_{th}	: Thermal unit ramp rates
P_{th}^{\min}	: Thermal unit minimum stable generation
P_{th}^{\max}	: Thermal unit maximum generation
λ_{ws}	: Maximum allowable wind spillage energy percentage in the system (weekly)
P_{ig}	: Inflexible generation in the system
Δt	: Duration of each time interval
T	: Number of total time intervals

I. INTRODUCTION

HIGH wind penetration is a key feature of future energy systems, driven by various energy and environmental policies. Denmark, Portugal and Spain are the top three countries, which have the highest percentage of annual wind generation with respect to their total electricity consumption [1]. In Denmark wind penetration level was about 30% of its annual electricity consumption in 2012 [1] and is expected to reach 50% by 2020 [2]. In the United States, five states with the highest installed wind capacity are Texas, California, Iowa, Illinois and Oregon [3]. Wind power contributed 3.5% of U.S. annual generation in 2012 [1].

High wind penetration results in two major challenges due to its variable and uncertain nature. These characteristics result in wind power forecast error and high ramp rates. Wind power variability requires more flexible generation in the system to increase power output when wind is not available or decrease power output when the wind output is higher than what the system can absorb. These challenges can be addressed by deploying large-scale energy storage systems.

Large-scale energy storage systems have high ramp rates and can be used to shift the excess wind energy from off-peak periods to peak periods. Energy storage sizing considering the total investment and operating costs as an objective function

has been studied in [4]-[5]. This optimization problem has also been considered to smooth out the combined power output of wind farms and energy storage in [6]-[9]. The impact of energy storage to improve the availability and reliability of renewable energy resources have been studied in [10]-[11]. The Electric Power Research Institute (EPRI) has published a report on Energy Storage Valuation Tool (ESVT) discussing costs and benefits of using energy storage in electric power systems [12]. The sizing of energy storage to mitigate the challenge of inflexible generation by base load power plants as coal and nuclear in a system with high wind generation has been proposed in [13]. A variety of heuristic methods and game theory approach have also been used to solve this optimization problem [14]-[17]. While utilizing the energy storage to mitigate the wind integration challenge has been extensively studied, there is still a need for an in-depth study.

The hybrid configuration of Compressed air energy storage (CAES) and Sodium Sulphur (NaS) battery is modeled in this paper. This paper presents a model for Compressed air energy storage (CAES) which takes into account its particular characteristic that requires minimum 20 minutes of idle time to switch between charging/discharging modes [19]. Other energy storage properties such as efficiency, ramp rates, power and energy capacity limits are also modeled for CAES and NaS battery.

The objective function in this paper is formulated to maximize the wind penetration level by changing the number of CAES and NaS battery units while taking into account the inflexible generation from existing thermal power plants (e.g., nuclear and large coal). These results may be of interest to those interested in developing large-scale storage facilities. This problem is formulated as a mixed integer linear programming (MILP) in CPLEX with time horizon of one year and 15-minute resolution.

Rest of the paper is organized as follows. Section II describes the system modeling. The case study and discussion are presented in section III. Section IV contains the conclusion.

II. SYSTEM MODELING

The entire system topology including the CAES, NaS battery, thermal unit, wind farm and load is presented in Fig. 1. The energy storage and thermal unit are modeled in details. The wind generation is considered as a negative load. In addition, the system operator also has a choice to curtail the wind while satisfying the weekly allowable maximum wind spill constraint. Transmission congestion is not considered in this paper.

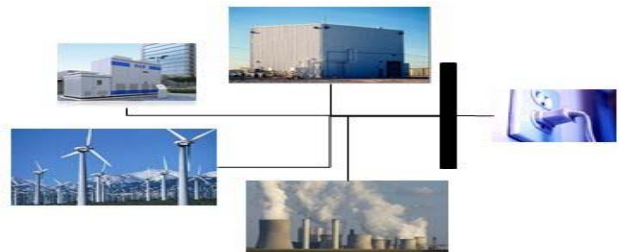


Fig. 1. The system topology

A. Objective Function

The objective function is to maximize the wind power scaling factor as presented in (1).

$$\max(\mu_w) \quad (1)$$

The objective function is simplified by considering the scaling factor as an unknown parameter to be multiplied by the historical wind power time series. Therefore, the intrinsic sequential characteristics of wind power can be considered. This objective function is beneficial for investors in wind power parks and energy storage sectors. The results give a limit of wind power absorption given the existing flexible and inflexible generation. Results also indicate the level of wind power that can be absorbed by increasing the number of energy storage units.

B. Constraints

The equality and inequality constraints to model the overall system are presented as follows. All constraints are applied for each 15-min time interval with weekly time horizon for the whole year.

Power balance constraint (2), which ensures that the total generation including the inflexible generation, thermal units, discharging power of energy storage units and wind power minus the wind spill power equal to the total load plus charging power of energy storage units at each time interval.

$$p_{l,t} = P_{ig} + \mu_w p_{w,t} + p_{th,t} + p_{Cdchg,t} - p_{Cchg,t} + p_{Ndchg,t} - p_{Nchg,t} - p_{ws,t} \quad \forall t \quad (2)$$

Constraints to model CAES and NaS battery, thermal units and allowable maximum wind spill energy are formulated as follows.

NaS battery is large-scale chemical energy storage and CAES is large-scale mechanical energy storage. Hence, they have different and sometimes mutually exclusive characteristics. The operation of both technologies has constraints as power and energy capacity, efficiency and maximum ramp up/down rates. NaS battery has 80% depth of discharge, meaning it can be charged till 90% full and discharged till 10% of the energy remains. On the other hand, CAES requires minimum 20 minutes idle time to switch between charging/discharging modes [20].

1) Compressed air energy storage modeling (CAES):

Refill constraint (3): This ensures that the final state of charge equals to the initial state of charge on a weekly cycle.

$$\sum_{t'}^{weekly} (p_{Cchg,t} \eta_C - p_{Cdchg,t}) \Delta t = 0 \quad (3)$$

Operation mode constraint (4): CAES can operate at one mode at a time only as charging, discharging and idle.

$$\alpha_{C,t} + \beta_{C,t} + \gamma_{C,t} = 1, \forall t \quad (4)$$

Charging/discharging power constraints (5)-(6): limits the operational power to the rated power of energy storage.

$$0 \leq p_{Cchg,t} \leq P_C N_C \alpha_{C,t}, \forall t \quad (5)$$

$$0 \leq p_{Cdchg,t} \leq P_C N_C \beta_{C,t}, \forall t \quad (6)$$

The relationship among start and stop indicators of idle

modes are represented as (7)-(8).

$$\rho_{C,t} - \varphi_{C,t} = \gamma_{C,t} - \gamma_{C,t-1}, t > 1 \quad (7)$$

$$\rho_{C,t} + \varphi_{C,t} \leq 1, \forall t \quad (8)$$

Required idle time constraint (9)-(11): The relationships between binary variables ensuring that if the mode of operation changes the CAES remain idle for T_C^{\min} .

$$\rho_{C,t} - \varphi_{C,t} = (\alpha_{C,t-1} - \alpha_{C,t}) + (\beta_{C,t-1} - \beta_{C,t}), t > 1 \quad (9)$$

$$-1 \leq (\alpha_{C,t-1} - \alpha_{C,t}) + (\beta_{C,t-1} - \beta_{C,t}) \leq 1, t > 1 \quad (10)$$

$$\sum_{t'=t}^{t+T_C^{\min}-1} \gamma_{C,t'} \geq T_C^{\min} \rho_{C,t}, \forall t \quad (11)$$

Energy capacity constraint (12): State of charge at each time interval is limited to the energy capacity of CAES.

$$0 \leq \frac{\sum_{t'=1}^k (p_{Cchg,t'} \eta_C - p_{Cdchg,t'}) \Delta t}{E_C N_C} + SOC_C^i \leq 1, k = 1 \dots T \quad (12)$$

Ramp rate constraint (13): Rate of change of storage output is limited to the storage ramp rate.

$$-dP_C N_C \leq \frac{(p_{Cchg,t} - p_{Cdchg,t}) - (p_{Cchg,t-1} - p_{Cdchg,t-1})}{\Delta t} \leq dP_C N_C, t > 1 \quad (13)$$

2) NaS battery modeling:

Refill constraint (14): This ensures that the final state of charge equals to the initial state of charge on a daily cycle.

$$\sum_{t'}^{Daily} (p_{Nchg,t'} \eta_N - p_{Ndchg,t'}) \Delta t = 0 \quad (14)$$

Charging/discharging power constraints (15)-(16): limits the operational power to the rated power of energy storage.

$$0 \leq p_{Nchg,t} \leq P_N N_N, \forall t \quad (15)$$

$$0 \leq p_{Ndchg,t} \leq P_N N_N, \forall t \quad (16)$$

Depth of discharge constraint (17): State of charge at each time interval is limited to the maximum and minimum state of charge.

$$SOC_N^{\min} \leq \frac{\sum_{t'=1}^k (p_{Nchg,t'} \eta_N - p_{Ndchg,t'}) \Delta t}{E_N N_N} + SOC_N^i \leq SOC_N^{\max}, k = 1 : T \quad (17)$$

Ramp rate constraint (18): Rate of change of storage output is limited to the storage ramp rate.

$$-dP_N N_N \leq \frac{(p_{Nchg,t} - p_{Ndchg,t}) - (p_{Nchg,t-1} - p_{Ndchg,t-1})}{\Delta t} \leq dP_N N_N, t > 1 \quad (18)$$

3) Thermal unit modeling:

Thermal unit is modeled by the following constraints.

Power constraint (19): operational power is limited to the maximum and minimum thermal unit power.

$$P_{th}^{\min} u_{th,t} \leq p_{th,t} \leq P_{th}^{\max} u_{th,t}, \forall t \quad (19)$$

Ramp rate constraint (20):

$$-dP_{th} \leq \frac{(p_{th,t} - p_{th,t-1})}{\Delta t} \leq dP_{th}, \forall t \quad (20)$$

The relationships among binary variables for thermal unit are presented in (21)-(22), to show the indicator of shutdown and startup of thermal units.

$$y_{th,t} - z_{th,t} = u_{th,t} - u_{th,t-1}, t > 1 \quad (21)$$

$$y_{th,t} + z_{th,t} \leq 1, \forall t \quad (22)$$

Thermal unit minimum up time constraint (23):

$$\sum_{t'=t}^{t+T_C^{\min}-1} u_{th,t'} \geq T_{th,up}^{\min} y_{th,t} \quad \forall t \quad (23)$$

Thermal unit minimum down time constraint (24):

$$\sum_{t'=t}^{t+T_C^{\min}-1} (1 - u_{th,t'}) \geq T_{th,dn}^{\min} z_{th,t} \quad \forall t \quad (24)$$

4) Other constraint:

The system operator has the choice to curtail the wind power. This constraint is presented by a maximum wind spill energy percentage for the time horizon of the simulation as in (25).

$$\sum_{t'=1}^T p_{ws,t'} \leq \lambda_{ws} \sum_{t'=1}^T p_{w,t'} \quad (25)$$

III. CASE STUDY AND DISCUSSION

The case study is based on the historical data from BPA in 2013 [18]. The peak load during the year is 10.64 GW. The installed wind capacity is 4.5 GW. The load, wind and net load (load minus wind) characteristics are summarized in Table I. The very small difference between the peak load and net load signifies that peak wind generation does not happen when the load peaks.

TABLE I.
BPA DATA CHARACTERISTICS

Unit	Max (GW)	Min (GW)	Max ramp up/down (GW/5min)	Mean (GW)	Sigma (GW)
Load	10.64	3.22	2.51/-2.48	6.28	0.93
Wind	4.5	0	0.80/-0.96	1.26	1.28
Net Load	10.20	0.87	2.48/-2.49	5.02	1.65

The optimization problem is independent for each week according to the daily and weekly refill of NaS battery and CAES. Hence, solving the problem for a week that has the maximum wind penetration is sufficient to find the maximum wind power scaling factor. According to the historical BPA data in 2013, last week of September has 37% wind energy penetration. Wind energy penetration is defined as the total wind energy produced during the whole week compared to the total energy consumed during that week.

The characteristics of each energy storage unit are shown in Table II. The initial state of charge for both CAES and NaS battery is assumed to be 0.5, meaning they can charge or discharge at the beginning. The inflexible generation in the

system is assumed to be 870 MW as the minimum net load presented in Table I. Thermal unit details are presented in Table III. The maximum capacity of the thermal unit is 10 GW to balance the maximum net load in the system.

TABLE II.
LARGE SCALE ENERGY STORAGE CHARACTERISTICS [19],[20]

Unit	Power (MW)	Energy (MWh)	Ramp rate (MW/min)	Efficiency (%)	DoD (%)	Idle Time (min)
NAS	50	300	50	70-90	80	--
CAES	300	6000	18	60-70	--	20

TABLE III.
THERMAL UNIT CHARACTERISTICS

Unit	Max power (MW)	Min power (MW)	Ramp rate (MW/min)	Min up/down time (hours)
THERMAL	10000	150	100	3

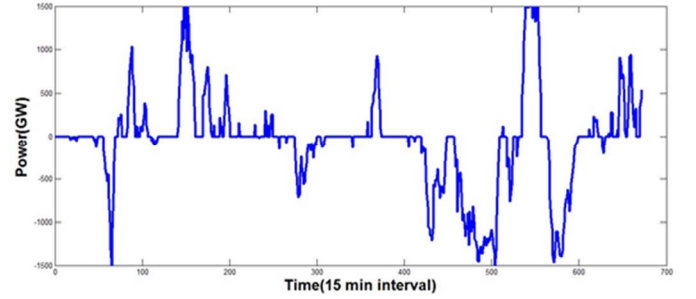


Fig.2. CAES operation for a week with 15 minute time interval

The CAES operation for 5 units of 300MW each derived from the linear programming results is depicted in Fig. 2. As one can observe, the required idle time constraint for transition between charging/discharging modes is satisfied. The wind power scaling factor results for different maximum allowable wind spill energy percentages are shown in Table IV and Table V, respectively.

TABLE IV.
OPTIMIZATION RESULTS FOR SCALING FACTOR FOR $\lambda_{ws} = 0\%$

CAES \ NAS	0	1	2	3	4	5
0	1.00	1.12	1.20	1.27	1.35	1.42
1	1.01	1.14	1.21	1.28	1.36	1.43
2	1.04	1.15	1.22	1.30	1.37	1.44
3	1.08	1.16	1.23	1.31	1.38	1.46
4	1.09	1.17	1.25	1.32	1.39	1.47

TABLE V.
OPTIMIZATION RESULTS FOR SCALING FACTOR FOR $\lambda_{ws} = 5\%$

CAES \ NAS	0	1	2	3	4	5
0	1.40	1.49	1.57	1.65	1.72	1.77
1	1.42	1.50	1.58	1.66	1.73	1.78
2	1.43	1.51	1.59	1.67	1.74	1.78
3	1.44	1.52	1.60	1.68	1.75	1.79
4	1.45	1.53	1.61	1.69	1.75	1.80

These results indicate that by increasing the number of CAES and NaS battery units, the wind power scaling factor increases. As shown in Table IV, by considering 0% wind spill percentage, the scaling factor for no energy storage unit is one since the inflexible generation is assumed to be minimum of the net load.

Table IV indicates that by increasing the CAES unit to 5

(equal to 1500MW CAES with 20 hours capacity) and 4 NaS battery units (200MW with 6 hours capacity) the scaling factor increases to 1.47. On the other hand, Table V, which allows 5% wind energy curtailment, shows 40% more wind power can be absorbed without any energy storage units. By installing 5 CAES unit and 4 NaS battery units, this number increases to 1.8 meaning that 80% more wind power can be absorbed while allowing 5% wind spillage.

Since the main problem to accept more wind power is the inflexible generation in the system, bulk energy storage is required to absorb the wind power rather than making the net load to be less than the inflexible generation. CAES and NaS battery are good candidates in large-scale energy storage units that can mitigate this problem due to its high capacity [19].

IV. CONCLUSION

High wind penetration requires more flexibility in electric power systems. This paper presents a detailed modeling for two types of large-scale energy storage units as flexible resources to increase wind energy penetration levels. The hybrid configuration of CAES and NaS battery is modeled in this paper. The CAES model presented in this paper considers the required idle time for charging/discharging mode transition in addition to efficiency, ramp rates, power rating and energy capacity.

The objective function presented in this paper is the scaling factor of wind power time series. Results indicate that by increasing the flexibility in the system as number of energy storage units, more wind power can be absorbed and extra wind farms can be planned.

Analyses in this paper are based on technical issues of power system and energy storage units. The economic evaluations are beyond the scope of this paper.

V. REFERENCES

- [1] "GWEC annual report 2012". Retrieved November 5., 2013, available online at http://www.gwec.net/wp-content/uploads/2012/06/Annual_report_2012_LowRes.pdf
- [2] "Energy comes together in Denmark", *IEEE power & energy magazine*, pp. 46-55, September/October issue 2013,
- [3] "Wind power in the United States", available online at http://en.wikipedia.org/wiki/Wind_power_in_the_United_States
- [4] H. T. Le, S. Santoso, and T. Q. Nguyen, "Augmenting wind power penetration and grid voltage stability limits using ESS: application design, sizing, and a case Study," *IEEE Trans. Power Syst.*, vol. 27, no. 1, pp. 161-171, Feb. 2012.
- [5] C. Abbey, and G. Joos, "A stochastic optimization approach to rating of energy storage systems in wind-diesel isolated grids," *IEEE Trans. Power Syst.*, vol. 24, no. 1, pp. 418-426, Apr. 2009.
- [6] S. Teleke, M. E. Baran, S. Bhattacharya, and A. Q. Huang, "Rule-based control of battery energy storage for dispatching intermittent renewable sources," *IEEE Trans. on Sustainable Energy*, vol. 1, no. 3, pp. 117-124, Oct. 2010.
- [7] L. Xu, X. Ruan, Ch. Mao, B. Zhang and Y. Luo, "An Improved Optimal Sizing Method for Wind-Solar-Battery Hybrid Power System," *IEEE Trans. on Sustainable Energy*, vol. 4, no. 3, pp. 774-785, July. 2013.
- [8] T. K. A. Brekken, A. Yokochi, A. V. Jouanne, Z. Z. Yen, H. M. Hapke, and D. A. Halamay, "Optimal energy storage sizing and control for wind power applications," *IEEE Trans. on Sustainable Energy*, vol. 2, no. 1, pp. 69-77, Jan. 2011

- [9] S. Teleke, M. E. Baran, A. Q. Huang, S. Bhattacharya, and L. Anderson, "Control strategies for battery energy storage for wind farm dispatching," *IEEE Trans. on Energy Conversion.*, vol. 24, no. 3, pp.725-732, Sep. 2009.
- [10] Y. Levron, J. M. Guerrero, and Y. Beck, "Optimal power flow in micro grids with energy storage," *IEEE Trans. Power Syst.*, vol. 28, no. 3, pp. 3226-3234, Apr. 2013.
- [11] D. Gayme, and U. Topcu, "Optimal power flow with large-scale storage integration," *IEEE Trans. Power Syst.*, vol. 28, no. 2, pp. 709-717, May. 2013.
- [12] P. Wang, Z. Gao, and L. Bertling, "Operational adequacy studies of power systems with wind farms and energy storages," *IEEE Trans. Power Syst.*, vol. 27, no. 4, pp. 2377-2384, Nov. 2012.
- [13] C. Wang, Z. Lu, and Y. Qiao, "A consideration of the wind power benefits in day-ahead scheduling of wind-coal intensive power systems," *IEEE Trans. Power Syst.*, vol. 28, no. 1, pp. 236-245, Feb. 2013.
- [14] M. Ghofrani, A. Arabali, M. Etezadi-Amoli and M. S. Fadali, "Energy Storage Application for Performance Enhancement of Wind Integration," *IEEE Trans. Power Syst.*, vol. 28, no. 4, pp. 4803-4811, Nov. 2013.
- [15] S. Teleke, M. E. Baran, S. Bhattacharya, and A. Q. Huang, "Rule-based control of battery energy storage for dispatching intermittent renewable sources," *IEEE Trans. on Sustainable Energy*, vol. 1, no. 3, pp. 117-124, Oct. 2010.
- [16] S. Mei, Y. Wang, F. Liu, X. Zhang, and Z. Sun, "Game Approaches for Hybrid Power System Planning," *IEEE Trans. on Sustainable Energy*, vol. 3, no. 3, pp. 506-517, July. 2012.
- [17] Sh. Mei, D. Zhang, Y. Wang, F. Liu, and W. Wei, "Robust Optimization of Static Reserve Planning With Large-Scale Integration of Wind Power: A Game Theoretic Approach," *IEEE Trans. on Sustainable Energy*, vol. 5, no. 2, pp. 535-545, April. 2014.
- [18] Historical wind data 2013 available online at <http://transmission.bpa.gov/Business/operations/Wind/default.aspx>
- [19] F. S. Barnes, J. G. Levine, *Large scale energy storage handbook*, by CRC Press, March 3, 2011.
- [20] R. Carnegie, D. Gotham, D. Nderitu, P. V. Preckel, *Utility Scale Energy Storage Systems, Benefits, Application, and Technologies*, by State Utility Forecasting Group, June 2013. Available online at <http://www.purdue.edu/discoverypark/energy/assets/pdfs/SUFG/publications/SUFG%20Energy%20Storage%20Report.pdf>

VI. BIOGRAPHY

Hamideh Bitaraf (S'11) received her B.S. and M.S. degrees from Electrical Engineering Department of Sharif University of Technology, Tehran, Iran, in 2010 and 2012 respectively. She is currently working toward the Ph.D. degree in Bradley Department of Electrical and Computer Engineering at Virginia Polytechnic and state university. She is a graduate research assistant at Advanced Research Institute Arlington, VA, USA, since 2012. Her research interests include energy storage, wind power, demand response, renewable energy, smart grid and optimization methods.

Haiwang Zhong (S'10-M'13) received his B.S. and Ph.D. degrees from Electrical Engineering Department of Tsinghua University, China, in 2008 and 2013 respectively, where he is currently working as a research associate. His research interests include generation scheduling optimization, demand response and electricity markets.

Saifur Rahman (S'75-M'78-SM'83-F'98) is the director of the Advanced Research Institute at Virginia Tech, Arlington, VA, USA, where he is the Joseph Loring Professor of electrical and computer engineering. He also directs the Center for Energy and the Global Environment at the university. In 2014 he is serving as the editor-in-chief of the IEEE Electrification Magazine.

Prof. Rahman served as the chair of the U.S. National Science Foundation Advisory Committee for International Science and Engineering from 2010 to 2013. In 2006 he served as the vice president of the IEEE Publications Board, and a member of the IEEE Board of Governors. He is a distinguished lecturer of IEEE PES, and has published in the areas of smart grid, energy efficiency, conventional and renewable energy systems, load forecasting, uncertainty evaluation, and infrastructure planning.